Pergamon

Journal of Insect Physiology 49 (2003) 31–44

Journal of Insect Physiology

www.elsevier.com/locate/jinsphys

Zinc is incorporated into cuticular "tools" after ecdysis: The time course of the zinc distribution in "tools" and whole bodies of an ant and a scorpion

R.M.S. Schofield [a,*], M.H. Nesson [b], K.A. Richardson [a], P. Wyeth [c]

[a] *Department of Physics, University of Oregon, Eugene, OR 97403,USA*
[b] *Department of Biochemistry and Biophysics, Oregon State University, Corvallis, OR 97331, USA*
[c] *University of Southampton Department of Chemistry, Southampton, UK*

Received 7 March 2002; received in revised form 26 September 2002; accepted 27 September 2002

Abstract

An understanding of the developmental course of specialized accumulations in the cuticular "tools" of arthropods will give clues to the chemical form, function and biology of these accumulations as well as to their evolutionary history. Specimens from individuals representing a range of developmental stages were examined using MeV - Ion microscopy. We found that zinc, manganese, calcium and chlorine began to accumulate in the mandibular teeth of the ant *Tapinoma sessile* after pre-ecdysial tanning, and the zinc mostly after eclosion; peak measured zinc concentrations reached 16% of dry mass. Accumulations in the pedipalp teeth, tarsal claws, cheliceral teeth and sting (aculeus) of the scorpion *Vaejovis spinigeris* also began after pre-ecdysial tanning and more than 48 h after ecdysis of the second instars. Zinc may be deposited in the fully formed cuticle through a network of nanometer scale canals that we observed only in the metal bearing cuticle of both the ants and scorpions. In addition to the elemental analyses of cuticular "tools", quantitative distribution maps for whole ants were obtained. The zinc content of the mandibular teeth was a small fraction of, and independent of, the total body content of zinc. We did not find specialized storage sites that were depleted when zinc was incorporated into the mandibular teeth. The similarities in the time course of zinc, manganese and calcium deposition in the cuticular "tools" of the ant (a hexapod arthropod) and those of the scorpion (a chelicerate arthropod) contribute to the evidence suggesting that heavy metal - halogen fortification evolved before these groups diverged.

Keywords: Cuticle; Biomineralization; Calcification; Deposit excretion; PIXE; STIM; Pre-ecdysial tanning; Manganese; Calcium; Chlorine; Halogens

1. Introduction

A large fraction of examined arthropods and many members of other phyla contain high concentrations of zinc, manganese, other heavy metals, or halogens in the contact regions of cuticular "tools" - jaws, leg claws and other implements for interacting with their environment (Schofield, 2001). We have recently shown that the hardness of the mandibular teeth of leaf-cutter ants, *Atta sexdens*, increases nearly threefold as zinc is incorporated during early adult life. Differences between the leaf-cutting behavior of young and older adults may be associated with this zinc-correlated hardness change (Schofield et al., 2002). The form of these accumulations is not yet known: although concentrations reaching 25% of dry mass have been measured (zinc in scorpion stings), the structures do not appear to contain a distinct biomineral phase like that found in the radula of mollusks or the cuticle of crustaceans. At the same time, zinc contents are often too high for the zinc atoms to be bound as individual ions to protein binding sites (Schofield, 2001).

In this paper we attempt to answer the question of when, in the course of cuticular development, zinc and associated elements accumulate. The time course of

* Corresponding author. Tel.:+1-541-346-4783; fax:+1-541-346-5861.
E-mail address: rmss@conch.uoregon.edu (R.M.S. Schofield).

0022-1910/03/$ - see front matter © 2003 Elsevier Science Ltd. All rights reserved.
doi:10.1016/S0022-1910(02)00224-X

accumulation has implications for the mechanisms of incorporation, the form and function of these accumulations, and questions of evolutionary origin, such as similarities to calcification systems. Preliminary investigations of pupal and recently emerged adult ants suggested that zinc might be incorporated into mandibles late in cuticular development (Grime et al., 1999, Schofield and Wyeth, unpublished results). We will show here that zinc incorporation begins between about 125 and 190 h after the beginning of pre-ecdysial darkening in both the ants and the scorpions that we examined. Darkening of cuticle is generally thought to occur at the same time as sclerotization, though they can be independent processes (Andersen et al., 1996; Hopkins and Kramer, 1992). Sclerotization, or hardening of the cuticle, is though to be one of the last steps in cuticular development. Darkening of cuticular "tools" occurs prior to darkening of the rest of the cuticle and before ecdysis in most arthropods. This has been described as pre-ecdysial tanning or pre-ecdysial hardening and is referred to here as pre-ecdysial darkening.

We also investigated the time course of accumulation of several other elements that are associated with zinc: cuticular implements enriched with zinc are often also enriched, to a lesser degree, with manganese, calcium and chlorine (Schofield, 2001). Within the structures, the spatial distribution of chlorine is tightly correlated with the zinc distribution while the highest concentrations of manganese and calcium are generally found in regions that have lower concentrations of zinc. The time course of deposition of these elements may offer clues to the biochemistry and reveal similarities between zinc fortification in different phyla.

In addition to time series of cuticular structures, we obtained time series of whole ants showing the distribution of zinc during the development of these ants. To our knowledge this is the first developmental time series showing directly the distribution of elements in entire organisms. We use these whole-body series to answer questions about the fraction of the organisms' zinc that is incorporated into the cuticle, any storage and redistribution of zinc prior to and during deposition and whether the zinc is inherited from earlier developmental stages or must be obtained from food.

2. Materials and methods

2.1. Specimens

2.1.1. Ants

Colonies of the odorous house ant, *Tapinoma sessile* (identification: Smith, 1965) were collected in two environments in the Willamette Valley, Oregon; colony 2 from an urban house, and colonies 1 and 5 from rotting Douglas fir poles on farmland. Once collected, colony 1 was fed on brown-sugar water and colonies 2 and 5 were fed on the ant food described below. In addition to the collected colonies, two sets of foragers were collected from other urban locations over a mile apart, identified as colonies 3 and 4. These ants were not fed and were frozen soon after collection.

Late stage pupae (P4–defined below) were isolated individually in 13×100 mm glass culture tubes. The tubes were horizontally oriented and about half filled with reverse-osmosis purified water held against the closed end of the tube by a glass-wool plug. For ants from colony 1, the water contained brown sugar. The culture tubes were then sealed with a second glass-wool plug and incubated at 28 (±1) degrees centigrade. The pupae were inspected at intervals, and the time of eclosion (the last ecdysis: escape of the pharate adult from the cuticle of the pupa) was set to be at the center of the time span between the first observation that eclosion had begun and the prior inspection time. Eclosion was defined as having begun if the tarsal–tibial joints of at least two legs were observed to be at least two joint widths from their locations in the pupal posture. Throughout this paper, "eclosion" will refer to this beginning of eclosion. The error bars for the time of eclosion were set to cover the time span between the two inspections. In some cases, about 0.01 ml of the ant food described below was placed in the culture tube and one or more "nurse ants" were placed in the tube with the specimen to assist with eclosion. The age-determined individuals from colony 2 were isolated as stage 3 pupae within a week of collection of the colony, and thus feeding prior to pupation was in the original environment. All data here are for worker ants.

Pupae were categorized visually according to the following features: P1: eyes and mandibular teeth light (not darker than in the lightest pupae (lasting about seven days)); P2: eyes darker than in lightest pupae but mandibular teeth not darker than the teeth of the lightest pupae (lasting about nine days); P3: eyes and mandibular teeth darker than in the lightest pupae (lasting about 3.5 days); P4: eyes, mandibular teeth and regions of abdominal cuticle dark (lasting about 2.5 days, until eclosion).

Ant food was prepared by blending 150 gms of analytical reagent grade sucrose (Malinckrodt Chemical, Paris, KY) with 50 gms of zinc deficient L-amino acid rat diet powder (preparation #515245, Dyets Inc., Bethlehem, PA) and 3.2 ml of 0.1M $ZnCl_2$, mixed together in reverse-osmosis purified water. The zinc content of this food was thus about 100 ppm of dry mass; typical zinc concentrations in fruit are in the 10–100 range of ppm by dry mass (Holland et al., 1996). Partial air-drying of the food before placing it in the culture tubes prevented ants from becoming entrapped.

2.1.2. Scorpions

Specimens of the scorpions *Vaejovis spinigeris* and *Centruroides exilicauda*, collected in Arizona, were obtained from Hatari Invertebrates (Portal, AZ). Some of the specimens produced litters which were separated in culture dishes, kept at 28 (±1) °C, and monitored for ecdysis as the ants above. The time of ecdysis (emergence from the old cuticle) of the second instars was set to be the time at which the second instars first stretched upward through the split exuvium as they began to pull their legs out of the exuvium.

First instars remain on the mother's back and so were not fed. The second instars of litter I were not fed, second instars of litter II were offered recently killed crickets.

2.2. Specimen preparation

Ant specimens were either air-dried after plunging them into liquid nitrogen, or, to preserve the gross structure of the internal soft tissue, freeze-substituted with acetone. Scorpion specimens were air-dried. For freeze-substitution the protocol of Fujita et al. (1987) was modified: 50 ml flasks were filled with about 20 ml of spectroscopy grade acetone and the flasks placed in liquid nitrogen until about half of the acetone was frozen. The flasks were then placed in a bed of dry ice and the specimens dropped into the liquid before the acetone ice on the sides and bottom of the flask had melted. The flasks were then placed in a styrofoam container filled with dry ice in a freezer maintained at about –30 °C. The dry ice lasted about three days and the specimens were left in the freezer for at least five days. They were then removed from the freezer, allowed to warm up to room temperature, filtered out of the acetone and air dried. After being epoxied to carbon fiber - epoxy pins, the specimens were placed in the vacuum of the microprobe target chamber.

Although we have previously determined that freeze-substitution does not detectably leach or redistribute iron, copper or zinc in the internal tissues of fruit flies (Schofield et al., 1997), we nevertheless examined air-dried ant specimens and found no significant difference in zinc content between air-dried and freeze-substituted whole adult bodies or mandibles, even during early stages of zinc incorporation. In addition, we found no significant difference between freeze-substituted and untreated pupae analyzed by atomic absorption spectroscopy (data not shown).

2.3. High-energy ion microscopy

Element contents were measured using a high-energy ion microprobe (Schofield, 2001). High-energy ion microprobes operate by focusing a beam of accelerated protons or other ions onto a specimen in a manner analogous to scanning electron microprobes. They have two major advantages over electron microprobes—namely, they provide lower element detection limits and, important here, greater tissue penetration (about 1 mm versus a few microns for electron probes). The beam passed through all specimens analyzed here. Because the accelerated particles can penetrate the specimen, their remaining energy can be measured (scanning transmission ion microscopy, STIM) in order to determine the total projected mass through which they have travelled; this mass measurement is used to normalize the element content obtained from the detection of emitted characteristic X-rays (particle induced X-ray emission, PIXE) and thereby produce concentration values. Because of the greater penetration of the ions, internal element distributions can be imaged. Although the accuracy of element quantification decreases for thicker specimens and for elements emitting lower energy X-rays, the uncertainty can be determined (Schofield and Lefevre, 1993). PIXE images for Na, Mg, Al, Si, P, S, Cl, K, Ca, I, V, Cr, Mn, Fe, Ni, Cu, Zn, As, Br and Sr X-rays were produced for every specimen examined here.

2.4. Scanning electron microscopy

Air-dried pedipalp fingers were sputter-coated with gold/palladium and examined at 20 KeV with an Amray 3300FE field emission scanning electron microscope.

2.5. Transmission electron microscopy

Transmission electron microscopy was performed with a Philips CM12 scanning transmission electron microscope, operated at either 40 or 60 KeV, equipped with an EDS 2000 energy-dispersive X-ray analysis system (IXRF Systems, Inc. Houston, TX).

Two protocols for sample preparation were utilized. When cellular preservation was required, freshly dissected cuticular structures were fixed in 2.5% glutaraldehyde, 2% paraformaldehyde, 0.1M Na cacodylate (pH 7.3), 1% sucrose, 0.16M $CaCl_2$ at 25 °C. for 4 h. After three buffer rinses, samples were dehydrated in a graded acetone series, infiltrated with Spurr's resin, and cured at 60 °C. for 24 h. Sections were generally examined unstained to allow X-ray analysis to locate metal-rich regions. For examination of canal arrangement within cuticle, air-dried specimens were dissected, structures of interest were rinsed briefly in 95% ethyl alcohol, infiltrated with Spurr's resin for 2–4 h, and cured for 24 h at 60 °C. Sections were usually examined unstained.

3. Results

3.1. Zinc incorporation into cuticular "tools" of Vaejovis

Specimens from two scorpion litters were examined in order to determine the time, relative to cuticular devel-

opment, at which zinc was incorporated into the cuticle. The cuticle of cuticular structures or "tools" of the second instars of these scorpions appeared to be fully formed beneath the cuticle of the first instars, more than 100 h before ecdysis. About 100 h before ecdysis, the cuticular "tools" of the second instars began to darken. By the time of ecdysis, the "tools" appeared to be fully darkened, although the surrounding cuticle continued to darken after ecdysis. We detected zinc enrichment only in specimens that were 90 or more h post-ecdysis (Table 1), about 190 h after the beginning of pre-ecdysial darkening. The high-energy ion microprobe images used in these investigations are demonstrated in Fig. 1.

The concentration of zinc in the distal tooth of the immovable finger of the chelicera of the 160 h old individual shown in Fig. 1 reached 5 (+/–0.6)% of dry mass (normalized using the mass data shown in the STIM image).

3.2. Scorpion pedipalp tooth ultrastructure

Detailed ultrastructural analysis of scorpion pedipalp teeth utilized both the zinc-enriched teeth of V. *spinigeris* and the zinc and iron-enriched teeth of *C.exilicauda*. The overall structural arrangements were the same for these two species.

Each examined pedipalp tooth (see Fig. 2) was associated with a large canal (~10 μm in diameter), filled with distinctive epidermal cells, that extended from the lumen of the pedipalp finger through the endocuticle toward the tooth. The canal terminated about 20–30 μm from the base of the tooth (Fig. 2B, C), at which point it transformed into a duct complex that penetrated an inpocketing of the inner exocuticle layer. The duct complex, in cross-section (data not shown), consisted of numerous 0.4 μm tissue-filled ducts within the invaginated inner exocuticle that extended from the distal end of the canal to the base of the modified outer exocuticle layer that comprises the metal-enriched part of the tooth (Fig. 2C). The ducts then ramified through the tooth matrix as 50–150 nm diameter ductules (Figs. 3, 4 and 6A), which, in some orientations, appeared to form roughly equidistant arrays (Fig. 3A, B). Both the ducts and the ductules clearly contained cellular processes, possibly microvilli-like extensions of the canal epidermal cells. The ductules appeared to connect to a complex of nanopores which ranged in diameter from 50 nm down to less than 5 nm (Figs. 3, 4 and 6A). The smaller nanopores were too narrow to contain membrane-bound cell processes, and, at least with the preparative methods employed so far, did not show any electron-dense fibrillar material, which is characteristic of exocuticular wax ducts.

The complexity of the arrangement of the nanopores within the matrix can be discerned in Fig. 4, which illustrates two mutually perpendicular orientations of pores from adjoining regions of a single section of a pedipalp tooth. The longitudinally oriented fine nanopores in Fig. 4B display an extremely regular parallel pattern with an interpore spacing of 17.5 nm. A full understanding of the exact interconnectedness of the pore complex will likely require a 3-D reconstruction prepared from serial sections. The fine nanopores extended to within 20 nm of the outer surface of the exocuticle, but did not appear to extend into the epicuticle layer (data not shown).

We could detect no differences in appearance of the cuticular ultrastructure between a fully zinc-enriched adult tooth (Fig. 3A) and that of a 38-h post-ecdysis second instar (Fig. 3B) that had not yet incorporated zinc into the matrix. We did not find a new layer or other ultrastructural features associated with zinc incorporation, or a biomineral phase distinguishable by electron density.

Table 1
Enrichment with zinc and associated elements was found only in the "tools" of second instar scorpions that were older than 48 h post ecdysis.

Litter[a]: Specimen	Hours after ecdysis (1^{st}–2^{nd} instars)[b]	Pedipalp	Chelicera	Tarsal claw			Sting		
		Zn	Zn	Zn	Mn	Ca	Zn	Mn	Ca
I:a	–176+/–5	–							
I:b	–149+/–5	–							
I:c	–79+/–5	–					–	–	–
I:d	2+/–0.5	–					–	–	–
I:e	38+/–2	–	–	–	–	–	–	–	–
II:a	48+/–0.5	–	–	–			–	–	–
I:f	90+/–0.5	Zn	Zn	Zn	**Mn**	**Ca**			
I:g	160+/–12	**Zn**	**Zn**	**Zn**	**Mn**	**Ca**	Zn	**Mn**	**Ca**
II:b	835+/–12	**Zn**	**Zn**	**Zn**			**Zn**	**Mn**	**Ca**

[a] Litter I was not fed, litter II was offered dead crickets.

[b] Negative ages are relative to the average time of ecdysis for litter-mates -: not enriched relative to surrounding tissue. Normal face: enriched, but in lower concentrations than the most enriched litter-mates (see Fig. 1). Bold face: enriched, percent levels. Empty cell: not investigated.

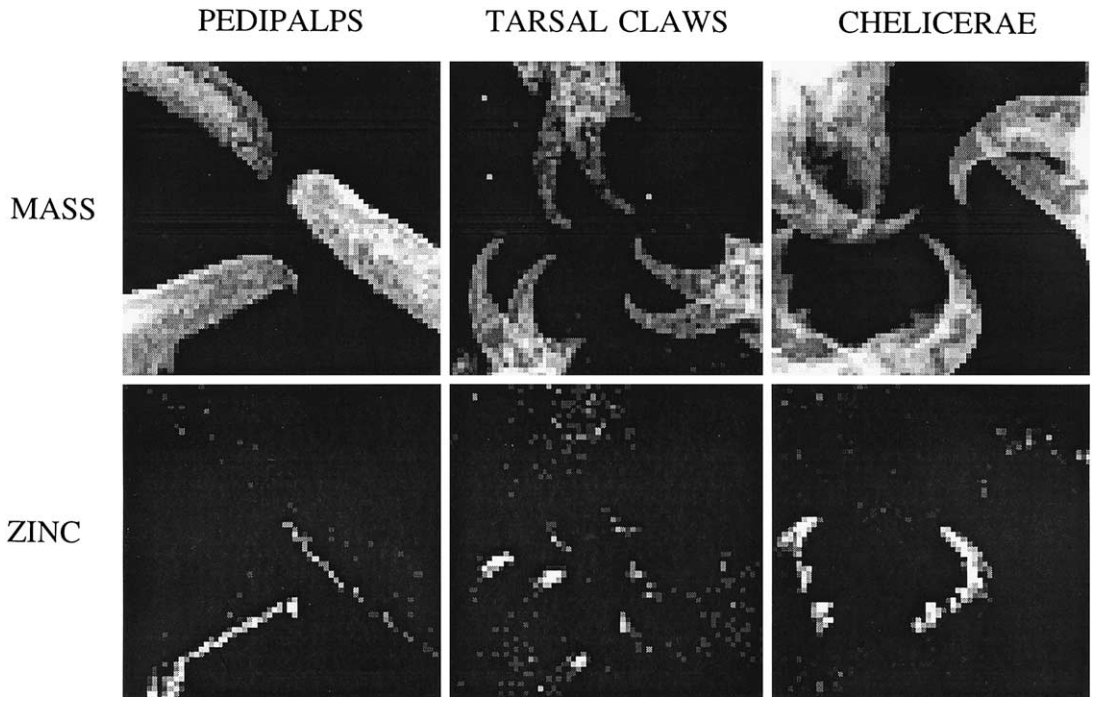

Fig. 1. Zinc incorporation into cuticular implements of developing second instar scorpions, *V. spinigeris*. Three specimens from litter mates of different ages are shown in each image; clockwise from the top left in each image, approximately 38, 90 and 160 h post-ecdysis. The images in the top row are STIM-derived, with lighter shades showing greater projected mass densities; below each of these images is a matching PIXE image showing the origin of zinc X-rays in nearly the same field, with lighter shades indicating greater numbers of X-ray counts. The first column shows pedipalp fingers, the second shows tarsal claws, and the third, chelicerae. The total zinc X-ray count (approximately proportional to content) for the distal 200 μm of the toothed regions of the pedipalps of the 38, 90 and 160 h old specimens was 9, 89 and 330 respectively; for the distal 50 μm of both lateral tarsal claws the count was 25, 38 and 214 respectively, and for the distal 50 μm of the right cheliceral finger the count was 18, 27 and 331 respectively. The frame edge lengths for the images of the pedipalps, tarsal claws, and chelicerae are, respectively, 1.1, 0.55 and 0.82 mm.

Nanopore arrays were absent from the zinc-free outer exocuticle layer immediately adjacent to the zinc-enriched pedipalp teeth (data not shown). We also examined the ultrastructure of a tooth-like, but zinc-free, protuberance present on the carina of the first metasomal segment of an adult *V. spinigeris* (Fig. 5). Upon comparison to the zinc-rich pedipalp tooth (Fig. 3A) at a similar magnification, the carina tooth outer exocuticle is nearly featureless, with no nanopores visible, and of homogeneous electron density.

A preliminary survey of other metal-enriched cuticular tools has revealed the occurrence of nanopore systems of varying degrees of complexity in: cheliceral teeth, tarsal claws and stings of scorpions; spider cheliceral fangs; ant mandibular teeth and tarsal claws (data not shown).

In the more basal region of a pedipalp tooth, where the zinc concentrations were lower than at the tip, we noted the occurrence of a pattern of zones of elevated electron density associated with individual nanopores (Fig. 6A). These dark zones are most readily discernable where they appear as rings around cross-sectioned pores, but it is likely that the numerous dark arcs and more linear features are also associated with out-of-plane nanopores. In the distal portion of the teeth, we have not observed such variations in electron density; we presume that in these areas of higher zinc concentration, the shells of elevated electron density surrounding each nanopore have grown centrifugally and have fused to produce a matrix of uniform electron density.

We have also observed a similar pattern of cuticular matrix of elevated electron density surrounding canals in the proximal region of the mandibular teeth of the ant, *T. sessile* (Fig. 6B). X-ray analysis of the ant tooth clearly demonstrated that the zones of higher electron density correlated closely with elevated zinc concentration (data not shown).

3.3. Zinc incorporation into cuticular "tools" of Tapinoma

Zinc incorporation into the mandibular teeth of the ant *T. sessile* also occurred after the teeth had darkened. The pupal stage in these ants typically lasted a little longer than 20 days. The mandibular teeth began darkening (defined as the beginning of P3) five or six days before eclosion (the last ecdysis). By the time of eclosion, the mandibular teeth appeared to be as dark as they were in older adults. Fig. 7 indicates that the zinc content of the mandibular teeth increased by a factor of about five dur-

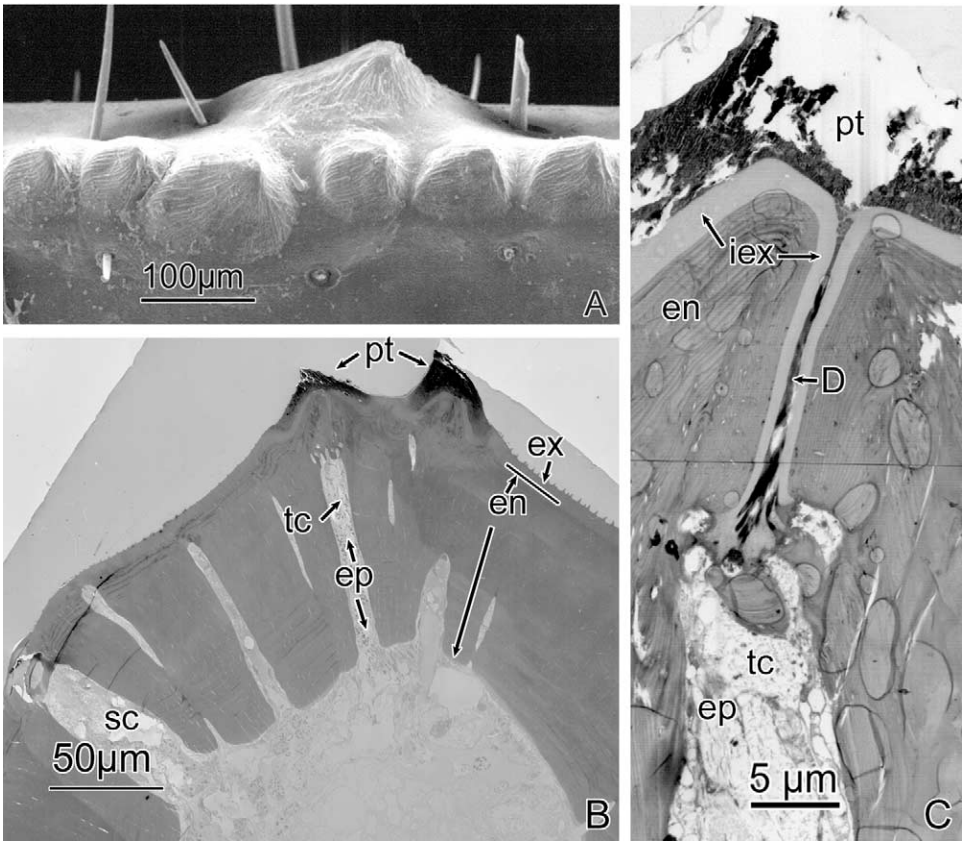

Fig. 2. (A) SEM image of several teeth on a scorpion pedipalp finger (*V. spinigeris*). Numerous sensory bristles border the main row of teeth and the auxiliary tooth. (B) TEM image of a cross-section of a scorpion pedipalp finger (*Centruroides exilicauda*) through the main row tooth and an auxiliary tooth. A tooth canal (**tc**), filled with specialized epidermal tissue (**ep**), extends through the endocuticle (**en**) from the lumen of the pedipalp toward the base of the tooth. The canal to the other tooth is out of the plane of the section. The Zn-enriched region of each tooth (**pt**) is distinguished by an increased electron-density and by a characteristic visual texture attributable to the sectioning properties of a material of increased hardness. The Zn-enriched layer appears to be a modified outer exocuticle. **sc**: canal associated with a sensory bristle. **C.** Higher magnification TEM image of the distal end of the same tooth canal (**tc**) from an unstained section close to that shown in Fig. 2B. Cellular material fills the duct complex (**D**), which extends to the base of the Zn-rich tooth matrix (**pt**), much of which has shattered during sectioning. The wall of the duct complex is formed from an invagination of the inner exocuticle layer (**iex**) that penetrates the endocuticle (**en**) to the distal tip of the tooth canal. **ep**: epidermal tissue. (B and C) glutaraldehyde/formaldehyde fixation, Spurr's resin, unstained.

ing the interval between 1 and 100 h after eclosion. For Fig. 7, data similar to those shown in Fig. 1 were used to produce content values for single mandibles from 14 individuals.

The curve plotted in Fig. 7 is an iterative fit to the mandible data based on a model in which zinc deposition begins abruptly and the deposition rate is proportional to the number of unfilled binding sites. For modeling, the single mandible values in Fig. 7 were doubled to account for both mandibles. The model gives the content of bound zinc in the mandibles

(Zn_{bound}) as: $Zn_{bound} = Zn_{max\ bound}(1 - e^{-(t - t_0)/\tau})$,

where "$Zn_{max\text{-}bound}$" is the bound quantity of zinc when all sites are filled in both mandibles, t is the time elapsed since eclosion, t_0 is the time at which binding began, and τ is the time constant. An iterative algorithm was used to fit the data in Fig. 7 to this model, giving values of 21 nanograms for $Zn_{max\text{-}bound}$, 41 h for τ, and –10 h for t_0 (deposition began 10 h before eclosion). A second, non-overlapping, data set consisting of mandible values for 16 different ants was also fit in order to assess the uncertainty in the above values (these data were derived from whole body images discussed below and are shown below in Fig. 9). The fit for this second data set, considered less accurate because mandibles in images of whole ants were analyzed instead of the higher resolution images of isolated mandibles used above, gave the following values: $Zn_{max\text{-}bound}$: 13 ngm; τ:67 h; t_0: –47 h. The fit for the primary data set gives an initial deposition rate of 0.51 ngm/h declining thereafter, with a rate of 0.39 ngm/h 1 h after eclosion. At a rate of 0.39 ngm/h, roughly 1% of the total body content of zinc must have been transported and bound in the mandibular teeth in one hour.

The concentration of zinc measured in the mandibular teeth of the colony 2 forager shown in Fig. 7 reached 16% of dry mass.

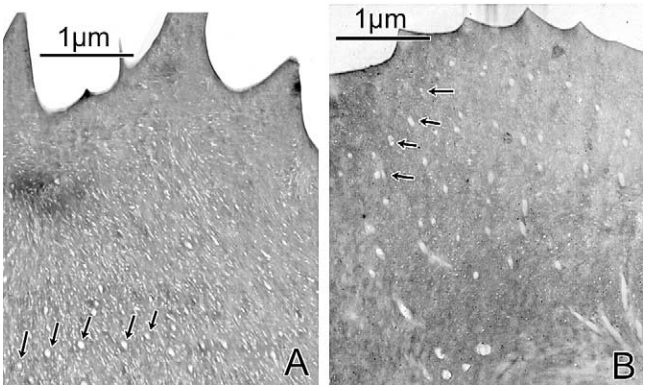

Fig. 3. After and before zinc incorporation. TEM images of sections, perpendicular to the conic axis of the tooth, through the distal ends of pedipalp teeth of *V. spinigeris*. The scalloped outer edges represent profiles through the ridges visible in Fig. 2 A. The arrows indicate ductules that arise from the duct complex at the base of the teeth. In some regions, the ductules occur in roughly equidistantly spaced arrays. Glutaraldehyde/formaldehyde fixation, Spurr's resin, unstained. (A) Adult female. (B) 38-h post-eclosion second instar (prior to zinc incorporation).

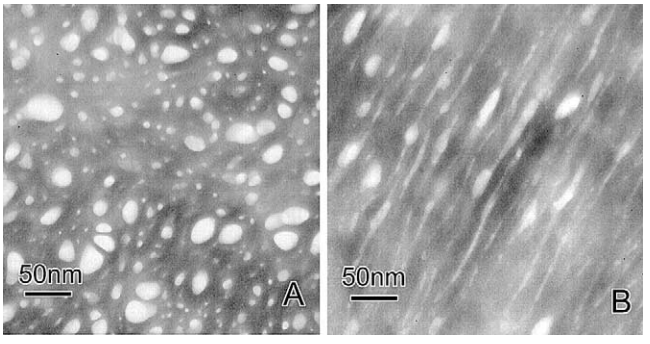

Fig. 4. (A and B) TEM images of two regions of the same unstained section of the distal region of a pedipalp tooth of an adult *V. spinigeris*, demonstrating both the complexity and the orderliness of the nanopore system that permeates the Zn-enriched matrix. Glutaraldehyde/formaldehyde fixation, Spurr's resin, unstained.

3.4. Incorporation of manganese, calcium and chlorine into cuticular implements

3.4.1. Manganese

Manganese accumulated before zinc in the examined cuticular implements (ants: mandibular teeth; scorpions: stings and tarsal claws—see Table 1). This accumulation sequence is demonstrated for the tarsal claws of Fig. 1 by X-ray spectra in Fig. 8. Because the mass, as determined by STIM, was similar for each of the tarsal claw specimens, the concentrations of zinc, manganese and calcium were approximately proportional to the X-ray peak heights. Early incorporation of manganese, relative to zinc, has also been reported in the mandibular teeth of the ant *Atta sexdens* (Grime et al., 1999, Schofield et al., 2002). In *Tapinoma*, manganese enrichment was observed in the mandibular teeth of eclosing individuals, though not in stage 3 pupae.

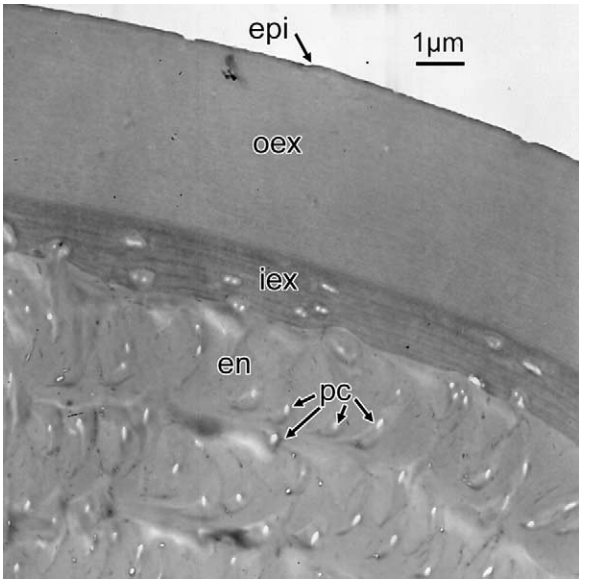

Fig. 5. Nanopores are not visible in a TEM image of a section through the sclerotised, but Zn-free, tooth-like protuberance on the carina of the first metasomal segment of an adult female *V. spinigeris*. **epi**: epicuticle; **oex**: outer (or hyaline) exocuticle; **iex**: lamellate inner exocuticle; **en**: endocuticle; **pc**: pore canals. Unfixed, Spurr's resin, unstained.

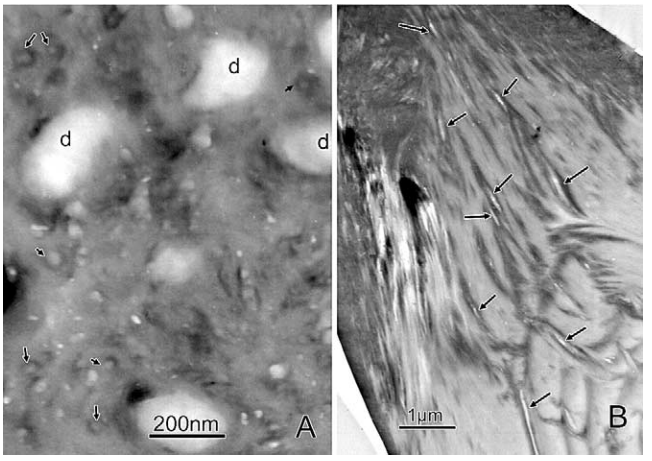

Fig. 6. (A) Elevated electron densities around nanopores; TEM image of a section of the basal region of a Zn-enriched pedipalp tooth of an adult *V. spinigeris*. Arrows indicate nanopores that are surrounded by cuticular matrix of elevated electron density, discernible as dark rings. Other electron-dense arcs and lines may be associated with out-of-plane nanopores, as well. (B) TEM image of an unstained longitudinal section through the second mandibular tooth of an adult *T. sessile* worker ant. Arrows indicate longitudinally sectioned pores bordered by zones of cuticular matrix that display elevated electron density. The tooth tip is beyond the top of the image**.** (A and B) glutaraldehyde/formaldehyde fixation, Spurr's resin, unstained.

3.4.2. Calcium

The tarsal claw data shown in Fig. 8 suggest that calcium accumulated before zinc and at the same time as manganese. This was also the case for the sting (see Table 1). Distribution maps of calcium in *Tapinoma*

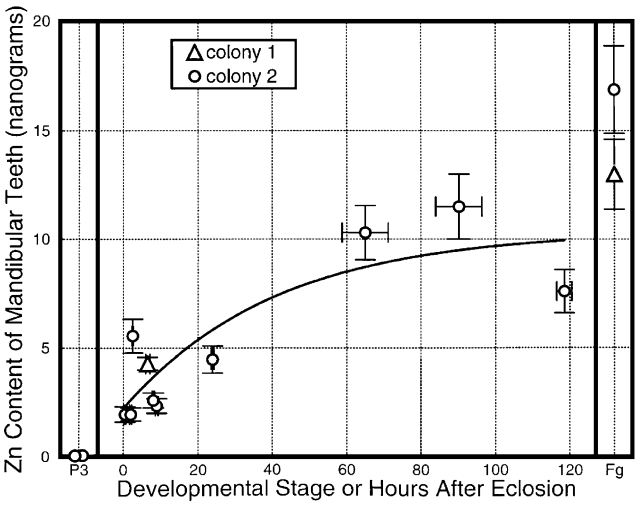

Fig. 7. The zinc content of ant mandibular teeth increases abruptly around the time of eclosion. The horizontal axis is labeled to indicate developmental stage (P3: pupal stage 3 [see Methods]; Fg: foragers—age not known but, because they were darkly colored and found foraging, they were thought to be older than the specimens identified by age). All contents are for single mandibles and were calculated from PIXE data such as that shown in Fig. 1. The mandibles were either freeze-substituted with acetone or air dried (values at 0.46, 2.0, 8.9, 23.8 and 119 h were obtained for air dried mandibles). The curve fitting the data for the mandibular teeth is based on the deposition model described in the text. Vertical error bars indicate a 68% confidence interval for the measured content of each individual specimen (Schofield and Lefevre, 1993); horizontal error bars give the time elapsed between the first observation of the beginning of eclosion, and the previous inspection.

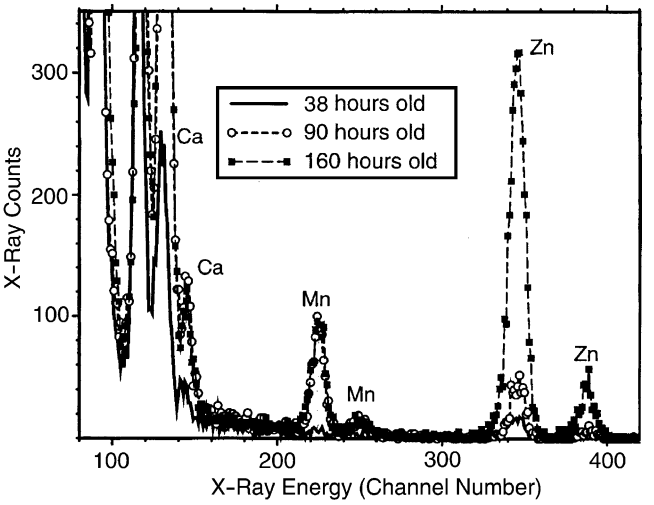

Fig. 8. X-ray spectra of the tips of tarsal claws (shown in Fig. 1) from 38, 90 and 160 h old second instar scorpion litter mates suggest that calcium and manganese are deposited before zinc. The two manganese and two calcium peaks are all several-fold larger in the 90 h individual than in the 38 h old individual but there is little difference between the 90 and 160 h old individuals (the lower-energy calcium peak is off-scale for the older two individuals). In contrast, the greatest count difference in the zinc peaks is between the 90 and 160 h old individuals. The data are consistent with a hypothesis that calcium and manganese are both deposited at the same time, prior to zinc deposition. The spectra for the three specimens nearly overlap in the valley between peaks at about channel number 100, evidence that specimens were otherwise similar. The measured calcium concentration in the 160 h specimen was about 0.7 (+/–0.1) % of dry mass, the manganese concentration was about 0.016 (+/–0.002) %, and the zinc concentration was about 3 (+/–0.4) % of dry mass (mass normalized by STIM).

mandibles (data not shown) were also consistent with simultaneous deposition of calcium and manganese before zinc.

3.4.3. Chlorine

Chlorine is difficult to quantify in these thick specimens because the low-energy chlorine X-rays are readily absorbed. However, the ratio of detected chlorine to sulfur X-rays (which are similarly attenuated) was at least ten times greater in the mandibular teeth of a 2-h post-eclosion *Tapinoma* specimen than in the teeth of a stage P3 pupa. Thus the chlorine and zinc levels appeared to increase together, though we were unable to quantify this observation.

3.5. The content and distribution of zinc in whole Tapinoma

3.5.1. Zinc content

In order to compare the content of zinc in the ant mandibles to that in whole bodies, the zinc content of the mandible region and of the whole body was calculated from PIXE data for whole ants. The results are plotted in Fig. 9. The zinc content of the mandibles was a minor fraction of the body content at all stages and ages [compare the total zinc content for each ant (filled symbols) to the mandible content (unfilled symbols) located directly beneath]. The average mandible zinc content of the foragers (right side of Fig. 9) was less than 1/10 of the average body content.

In addition to showing that the mandibles contain a small fraction of the total body zinc, Fig. 9 shows that the fractional variation between the mandible content of different individuals was much smaller than the variation in total body content. For example, the body contents of the six foragers on the right side of Fig. 9 vary by about a factor of 10 while the mandible contents vary by a factor of only 2. Furthermore, Fig. 9 shows that body content and mandible content are not well correlated; the ants with the greatest body content do not also have the greatest mandible content.

It is unlikely that the ants of Fig. 9 were either all overfed or all underfed zinc because of the variety of wild and laboratory diets. The foragers from colonies 3 and 4 were frozen immediately after collection and so represent two different wild diets. After collection, colonies 2 and 5 were fed on the ant food described in the Materials and Methods section. Colony 1 was fed on brown-sugar water after collection. The zinc contents of even the laboratory colonies were probably influenced

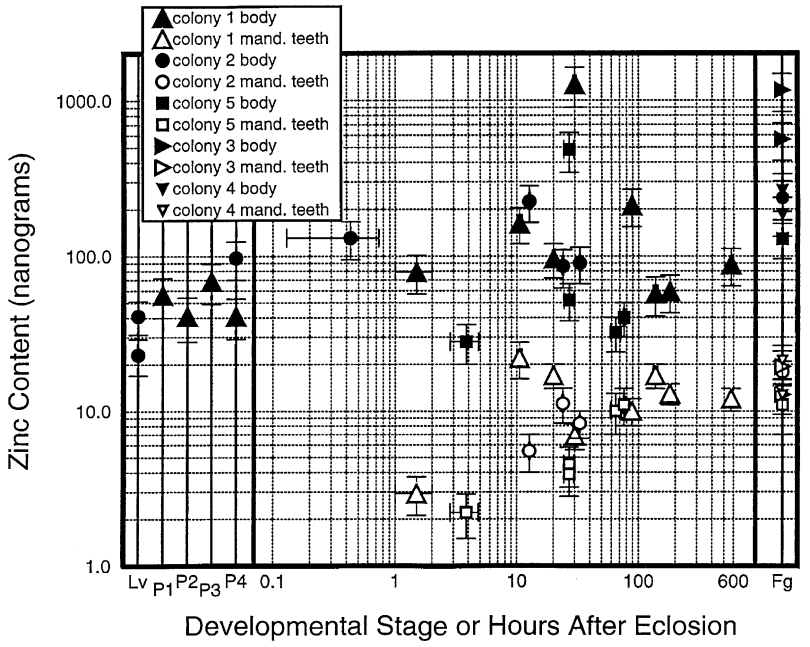

Fig. 9. The zinc content of whole ant bodies is much greater than the mandible content at all stages, and is more variable than and does not correlate with the mandible content. The horizontal axis is labeled to indicate developmental stage (Lv: larvae; P1, P2, P3 and P4: pupal stages [see Methods]; Fg: foragers—age not known but, because they were darkly colored and found foraging, they were thought to be older than most of the specimens identified by age). The mandible (both mandibles are included: unfilled symbols) and body (filled symbols) content of each individual can be compared because they align vertically according to age or stage. Values were calculated from PIXE data for whole specimens (see Fig. 10) that were freeze substituted with acetone. The mass of the 573 h old ant was 99,000 ngm (determined by STIM) so the average body concentration was about 0.089% of dry mass. Vertical error bars indicate a 68% confidence interval for the measured content of a single specimen (Schofield and Lefevre, 1993); horizontal error bars give the time elapsed between the first observation of the beginning of eclosion, and the previous inspection.

by diets in the wild because the colonies were in the laboratory for only a short period (one week to two months) before specimens were taken or pupae were isolated for timing, and because the larvae feed on material regurgitated from nurse ants during the two or three week long larval stage (Smith, 1928).

The high zinc content appeared to be roughly constant, not accumulative. Regression analysis of the data for the 17 whole bodies of known ages in Fig. 9 gave a slope of –0.29 ngm/h with a standard error of 0.56, while the slope expected for a linear increase in zinc content was about 1.63 ngm/h (calculated as the ratio of the difference between adult and pupal averages to the average adult age in the data set). The slope expected for a linear increase falls outside of the 0.995 confidence interval. This confidence interval was exceeded even when the two individuals with the highest zinc content and the 570 h old individual were excluded.

3.5.2. Zinc distribution

The PIXE images of whole developing ants allowed us to investigate the possibility of zinc redistribution during development and during incorporation of zinc into the mandibular teeth. Fig. 10 shows the distributions of mass and zinc in the abdomen and head regions of the ants whose total zinc contents are plotted in Fig. 9 as the colony 1 series. At all stages and ages shown in Fig. 10, zinc was distributed fairly uniformly throughout the body with localized accumulations in the midgut region, the mandible region of the adults, and the infrabuccal pocket region of several specimens. In the specimens containing the most zinc, the content of zinc in the abdomen was higher than in other regions.

A dispersed distribution of zinc was observed in *T. sessile* at all developmental stages from each colony. Zinc was distributed in high concentrations throughout the bodies of these ants, accumulating even in the legs. In contrast, zinc in fruit flies has been shown to be highly localized in the Malpighian tubules (Schofield et al., 1997).

The pattern of zinc accumulation in the midgut region has been previously noted for a different ant species (Schofield et al., 1988); the zinc was found to accumulate in tissue immediately surrounding a dissected midgut, either in the gut wall or in the surrounding Malpighian tubules, and was not in the contents of the midgut (Schofield, 1990). Similar concentrations (about 0.5% of dry mass) of zinc were found in the Malpighian tubules of fruit flies (Schofield et al., 1997). The Malpighian tubules of ants and flies may be involved in regulating zinc.

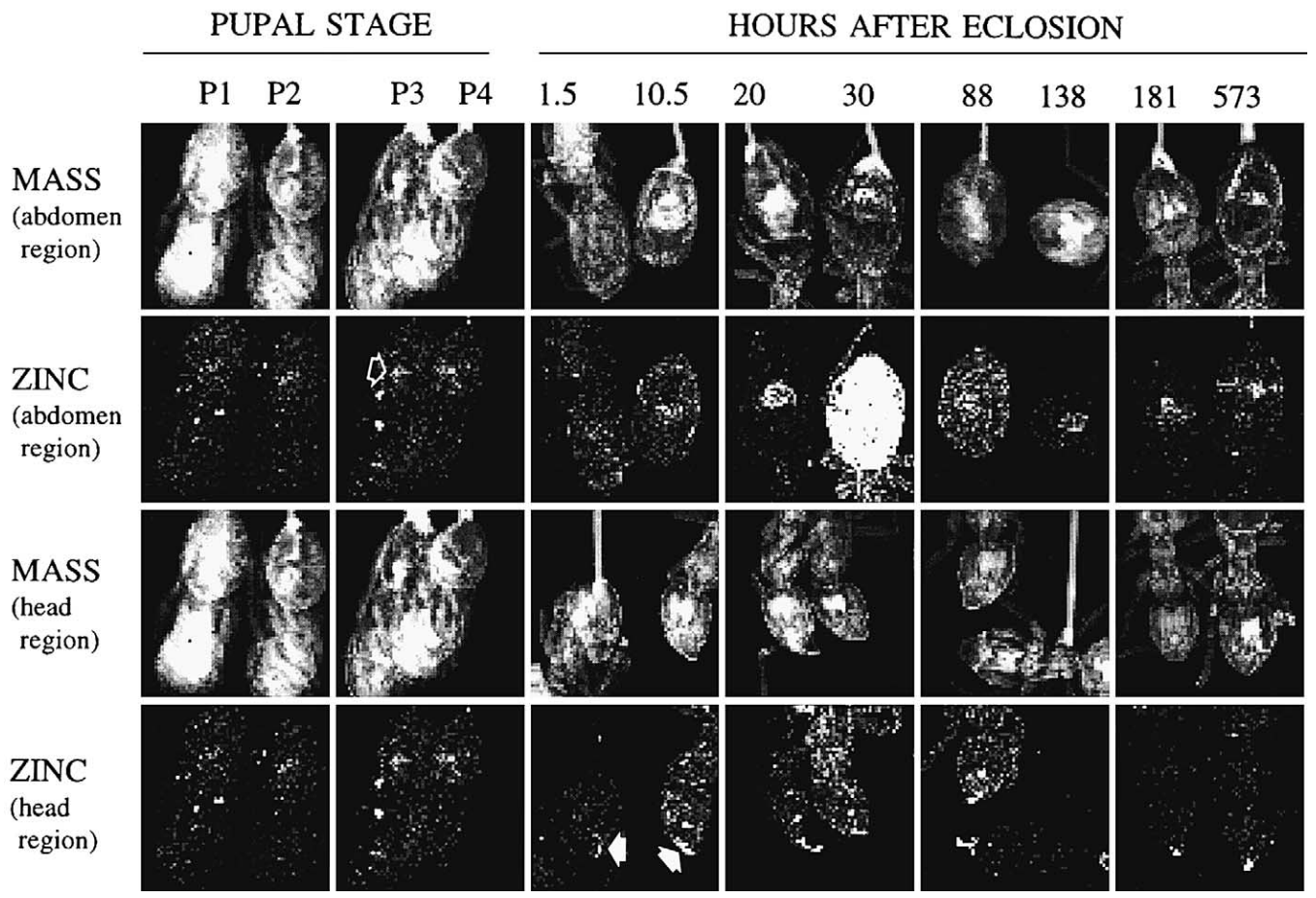

Fig. 10. Zinc is dispersed throughout the body with slightly higher levels in the midgut region, before, during and after development of mandibular accumulations in the ant *T. sessile*. Each square image in this mosaic is a 64×64 pixel STIM-derived (approximate projected mass density) or PIXE (approximate projected zinc density) image, showing the abdominal regions (top two rows) or head regions (bottom two rows) of two specimens. Pupal specimens are repeated in the top and bottom rows because pupae fit within the scan range of the probe. Each specimen appears four times, aligned in a column labeled at the top by its stage or age. A single grey scale is used for all zinc images so that a particular shade indicates a certain range of X-ray counts (and thus similar zinc content) in all images. This grey scale was set to maximize contrast in low zinc content regions where 0–14 X-rays per pixel were detected: white pixels indicate that 15 or more X-rays were detected (the highest X-ray count was 150). Grey scales for the different mass images are not uniform. The period of most rapid zinc incorporation into the mandibles is demonstrated in the head region image of the 1.5 and 10.5 hour old specimens (filled arrows point to the mandibles). The white spot an arrow length above the mandibles of the 10.5 h specimen corresponds to the infrabuccal pocket, which is zinc-rich and evident above the mandibles of the 20, 30 and 88 h old specimens as well. The zinc-enriched mid gut region is visible as a zinc-bright circular region near the center of each abdomen. As an example, it is indicated by an open arrow in the second row image of the P3 pupa. Beneath this arrow are two zinc-bright spots associated with particles of unknown origin on the surface of the P3 pupal case. Similar zinc-rich particles appear in several other places and were not included in the PIXE based calculation of zinc content for Fig. 9. The zinc content of the 30 h old ant (colony 1) was about ten times greater than that of other colony members (see plotted values in Fig. 9). Fig. 9 also shows that a 27 h old adult (colony 5) also contained almost ten times as much zinc as its peers. The source of this variation in not understood, though it does not appear to be associated with the technique (e.g. ants were imaged in pairs). The zinc content did not appear to be correlated with the presence of nurse ants in the isolation tube (e.g. the 30 h colony 1 individual had nurse ants, the 27 h colony 5 individuals did not). Individual frame edge: 2.2 mm.

4. Discussion

4.1. Incorporation of zinc late in cuticular development

The already-formed mandibular teeth of the ant pupae began darkening about 150 h before eclosion. Prior to eclosion, manganese and calcium concentrations increased relative to surrounding cuticle by up to several milligrams per gram of dry mass. Approximately 10 h before the beginning of eclosion, zinc deposition in the mandibular teeth began abruptly and was consistent with a model in which it followed a roughly exponential approach (with a time constant of about 40 h) to the fully enriched content. During the period of zinc incorporation, the mandibular teeth also became enriched with chlorine.

In the vaejovid scorpion, zinc was deposited beginning about 150–190 h after the beginning of pre-ecdysial darkening, and beginning about 50–90 h after ecdysis.

The time evolution of manganese and calcium accumulations was similar to that in the ants, in that they were mainly deposited prior to zinc. It was not clear whether or not chlorine was deposited at the same time as zinc, as in the ants.

The lateness of the process of zinc deposition into the cuticular matrix, after the cuticle has formed and darkened, would seem to require the presence of a pathway for the transport of zinc-containing precursor materials to the deposition site. Our ultrastructural studies demonstrate that there is a complex of 'plumbing' in the scorpion pedipalp teeth that develops before zinc deposition and could provide a direct connection from the epidermal cells that fill the tooth canal, through the tissue filled ducts and ductules, and then via the presumptive fluid filling the nanopores to the locus of deposition within the presumably specialized outer exocuticle matrix. Although we do not yet have a clear understanding of the chemistry and biochemistry of the zinc-enrichment process, the structural modifications, especially the extremely close spacing of the nanopores, suggest that the zinc-containing transport precursor must have an extremely limited diffusion path, within the already heavily sclerotized tool cuticle to reach the deposition end-site.

The sudden onset of deposition late in cuticular development suggests either that an active zinc transport system turned on or that the cuticle matrix was modified late in development to incorporate zinc, or both. It seems likely that an active pumping system was involved since, in the ants, about 1% of the body content of zinc (and a greater fraction of the mobile zinc) must have infiltrated the sclerotized cuticle of the mandibular teeth in one hour.

In both the ants and the scorpions, zinc and the other cuticle-enriching elements were mobilized from internal stores. This is evident because the ants and scorpions developed enriched cuticular structures before they were fed.

4.2. Similarities and differences between zinc fortification and calcification

The time course of zinc fortification in the ants and scorpions examined here is similar to that of calcification in crustaceans (Roer and Dillman, 1993). In consideration of a hypothesis that there is an evolutionary relationship between zinc fortification and calcification processes, we discuss some similarities and differences below. To begin with, three similarities will be considered: first, deposition late in cuticular development with similar deposition time constants; second, increased canal densities that may be associated with this late deposition; and third, a zinc–calcium association in both systems.

Like zinc deposition in the ants and scorpions studied here, calcium deposition in the crustacean cuticle takes place mainly after ecdysis, late in cuticular development. It seems likely that any late modification of the cuticle, with the resulting access difficulties, requires a more complex system than would fortification as the cuticle was being formed. Calcification may occur after ecdysis so that the cuticle can expand to accommodate growth of the crustacean before the cuticle becomes calcified. A growth-allowing adaptive advantage is not evident for post-ecdysis deposition of zinc in cuticular implements. In addition to the lateness of deposition, the time spans of the deposition periods are also similar: calcium concentration data for developing crustaceans, compiled by Roer and Dillman (1993), was fit using the above deposition equation, giving deposition time constants of about 10–20 h, compared to about 40 h for zinc in *Tapinoma*.

Whether or not there is an adaptive advantage associated with late zinc deposition, it is possible that parts of systems needed for late modification of the cuticle, such as canals, are evolutionarily related. Both calcified crustacean cuticle and zinc-fortified cuticle contain higher canal densities than unenriched cuticle. Higher canal densities in calcified cuticle, relative to uncalcified cuticle, have been observed in crustaceans (Compere and Goffinet, 1987a; Compere and Goffinet, 1987b). Further ultrastructural comparisons between canals associated with calcification and canals associated with zinc fortification are needed to investigate the possibility that the canals in the two systems are homologous.

In a wide variety of organisms, there is a zinc–calcium association: zinc often accumulates in small quantities in calcified tissue, and structures that are predominantly zinc-enriched are often also enriched with calcium. Zinc accumulates preferentially in the regions of primate bone undergoing mineralization (Guggenheim and Gaster, 1973), zinc has been found in 0.1% of dry mass concentrations near the tip of calcified hagfish teeth (Schofield, 1990), in concentrations approaching 10% of dry mass in the calcified stylets of nemertians (Schofield, unpublished data), and zinc accumulates at about the same time as calcium biominerals in the magnetite-filled teeth of chitons and in the same region as calcium in goethite-filled teeth of limpets (Webb et al., 1989). In structures that are predominantly zinc-enriched, the calcium concentration is often also elevated, usually in association with manganese (Schofield, 2001).

Notwithstanding these similarities, there are major differences between the calcium and zinc fortification systems that suggest that if parts of the two systems are related, they are not slight modifications of each other. Below, we discuss three differences: a three-fold greater number density of calcium atoms than zinc atoms, bromine rather than calcium enrichment in the cuticular "tools" of calcified crustaceans, and enrichment of different cuticular layers.

The concentration of calcium in crustacean cuticle is

typically about 25–35% of dry mass (Roer and Dillman, 1993; Vincent, 1982), while the measured zinc concentration reached about 16% of dry mass in the distal-most teeth of the colony 2 forager shown in Fig. 7. The number density of zinc atoms in the ant cuticle was thus about 0.34 of the number density of calcium atoms in typical crustacean cuticle. If the zinc were bound as a biomineral, the volume that the mineral filled would be smaller than the volume filled by $CaCO_3$ in crustacean cuticle—unless the zinc were a much smaller fraction of the biomineral molecule than calcium is of $CaCO_3$. Elemental analysis and EXAFS (Extended X-ray Absorption Fine Structure) analysis have eliminated most of the common zinc minerals, except possibly an amorphous ZnO, as candidates; apparently, only organic zinc salts could fill fractions of cuticle comparable to those filled by inorganic calcium salts in crustaceans (Schofield, 2001).

A second difference lies in the type of cuticular features that are fortified. Calcium enrichment does not necessarily substitute for heavy metal - halogen enrichment in cuticular "tools" of calcified arthropods. For example, near the tips of the tarsal claws of the calcified millipedes, crabs and isopods that we examined, calcium levels dropped and, instead, the predominant inorganic element was, in millipedes, chlorine, and in crustaceans, bromine (Schofield, unpublished data). It is possible that bromine enrichment modifies mechanical properties in a manner similar to zinc enrichment and differing from calcification. Heavy metal - halogen fortification may be preferable to calcification in the tips and edges of cuticular implements.

In addition to differences in the types of cuticular features that are calcified or zinc-fortified, there appear to be differences in the enriched cuticular layers. Zinc fortification occurs primarily in the exocuticular layer in the scorpions, while calcification in crustaceans is found in the epicuticle, the exocuticle, and the endocuticle (Roer and Dillman, 1993).

While the molecules that bind zinc in fortified cuticle do not appear to be organized in a crystal structure (both X-ray and electron diffractometry have not yielded diffraction patterns (Schofield, 2001)), this does not appear to be a significant difference with calcification. Amorphous calcium carbonate and phosphate are fairly common in crustacean cuticle (Lowenstam and Weiner, 1989).

It is preliminary to draw conclusions about any evolutionary relationship between calcification and heavy metal–halogen fortification systems from the similarities and differences discussed above. The lateness and time course of zinc incorporation, and the associations between calcium and zinc in both calcification and zinc fortification systems suggest that parts of the systems are similar and that they may be evolutionarily related. On the other hand, the differences between heavy metal–halogen and calcium fortification, in particular the lower number densities of zinc, and the differences in enriched features and cuticular layers, suggest that the two systems may modify mechanical properties in very different ways and that the biochemistry may be very different.

4.3. The low zinc content of the ant mandibles relative to total body content

Zinc fortification is unlikely to be a great additional energetic cost for the examined ants. The tens of nanograms of zinc in the mandibular teeth were roughly an order of magnitude less than the total body content of zinc in the adults, and less even than the variations in zinc content between individuals. This suggests that the extra cost in obtaining zinc for the mandibular teeth is small compared to the total expense of obtaining zinc. Even the pupae contained several times more zinc than necessary for the fully enriched mandibular teeth and, by the same argument, the extra cost for the nurse ants to provide zinc for mandibular teeth would be relatively small. The small quantity of zinc required for the mandibular teeth, relative to the total body content of zinc and to the variation in body content, argues against a hypothesis that zinc incorporation is delayed because it is costly to acquire.

4.4. Whole body zinc content and distribution

Deposit excretion, which would be expected to produce a roughly linear increase in zinc content with time, is not supported by the ant data here. We have previously noted that the zinc and copper contents of fruit flies are relatively independent of the metal concentration in their food and thus fruit fly data was also inconsistent with deposit excretion (Schofield et al., 1997). It appears that the high zinc levels in the ant and fly bodies were a result of regulated storage rather than deposit excretion. Zinc is an essential component of more than 300 enzymes and transcription factors (Coleman, 1992). Yet the total zinc content in these molecules is probably a small fraction of the body zinc content, and it is surprising that such large stores of zinc would be needed. It may be that the zinc excretion rate does not exceed the accumulation rate until toxic levels are approached, and so more zinc than necessary is accumulated.

The overall distribution patterns of zinc in whole *Tapinoma* bodies were independent of pupal stage or age, except in cuticular implements. The highest concentrations of zinc, outside of those in the cuticular implements, appeared to be in the region surrounding the midgut (which includes the Malpighian tubules) in pupae and adults.

4.5. Evolution

We suggest three possible evolutionary precursors of heavy metal–halogen fortification, which are not neces-

sarily mutually exclusive: a biomineralization system such as calcification, an organic cross-linking system such as that hypothesized for cuticle sclerotization, or a trace element transport and storage system that might not be associated with mechanical properties. Of the first two suggested precursors, the developmental course of the zinc system is more similar to the calcification system than it is to the sclerotization system. The third precursor is suggested because the ability to obtain, transport, store and regulate large quantities of zinc is well developed in the ants here and in fruit flies that do not have zinc-enriched cuticular structures (Schofield et al., 1997). This system for handling quantities of zinc that, in *T. sessile*, are much greater than those found in cuticular accumulations, may have predated heavy metal–halogen fortification and may have required little modification for zinc procurement, transport to, and perhaps even deposition in cuticular "tools".

The detailed similarities in zinc fortification systems between distantly related phyla suggest to us a very early origin of heavy metal–halogen fortification. For example, we have previously noted that the spatial distributions of zinc, chlorine, manganese and calcium accumulations in the jaws of a nereid worm are similar to the spatial distributions of these elements in cuticular "tools" of scorpions (Schofield, 2001). To these similarities in the elements that accumulate and in their spatial distributions, the present paper adds similarities in the time course of these accumulations in two distantly related arthropods. In both the ant (a hexapod arthropod) and the scorpion (a chelicerate arthropod), zinc fortification took place very late in cuticular development, and zinc was deposited after calcium and manganese. These developmental similarities further strengthen the argument that heavy metal–halogen fortification arose before these groups diverged.

5. Conclusions

1. Zinc was incorporated into the cuticle late in cuticular development, beginning about 125–150 h after the start of pre-ecdysial darkening (and predominantly after eclosion) in the ant *T. sessile*, and beginning between about 150 and 190 h after pre-ecdysial darkening began (and more than about 50 h after ecdysis) in the second instars of the scorpion *V. spinigeris*.
2. Manganese and calcium were incorporated prior to zinc in both the ant and the scorpion. At least in the ant, chlorine was incorporated at the same time as the zinc.
3. No differences in ultrastructural features were observed between TEM images of scorpion cuticle just before and after zinc incorporation.
4. In both the ant and the scorpion, zinc was distributed uniformly throughout the metal-bearing cuticle. Any granularity associated with a separate zinc-containing phase was limited in size to less than a couple of nanometers, the resolution of our TEM images.
5. In both the scorpions and the ants, the metal-bearing portion of the cuticle was filled with nanometer-scale canals. These canals were not present in adjacent non-metal-bearing cuticle or in cuticle of other teeth-like features that were not metal enriched. Near the boundary of the zinc-enriched regions, the cuticle immediately surrounding the canals was electron dense and contained the highest concentrations of zinc. This suggests that the zinc is incorporated into the already formed cuticle through this network of canals.
6. The detailed developmental and structural similarities between zinc fortification in the ant and the scorpion, along with the widespread phylogenetic distribution of these features (Schofield, 2001) suggest to us that this system evolved before these groups diverged.
7. There appeared to be an optimal or maximum mandibular zinc content that was reached in all ants within the incorporation period (about 100 h), notwithstanding the large variation in body zinc content. After the incorporation period, the zinc contents of the ant mandibles did not appear to increase and were similar between individuals, even though the body contents varied greatly.
8. The energetic expense of acquiring zinc for the ant mandibles appeared to be small relative to the total expense of acquiring zinc, because the fraction of zinc in the mandibles was small compared to the body content of zinc.
9. The body zinc content of the ants did not increase in a manner consistent with deposit excretion.
10. No localized regions for specialized storage of zinc prior to the rapid incorporation into the ant mandibles were observed. The midgut contained somewhat elevated zinc levels, but these levels did not appear to be higher before or lower after zinc incorporation into the mandibles. The zinc for the mandibles may come from the storage sites dispersed throughout the ant bodies.
11. Similarities between calcification and zinc-fortification suggest that at least parts of the two systems may be genetically related, but there are also major differences suggesting that, if they are related, the calcification and zinc-fortification systems are not just slight modifications of each other.

Acknowledgements

This work was supported by NSF grant IBN 9817206. We would like to acknowledge helpful discussions with

C. Jackson. A. Beiderwell, W. Teichman, and K. Hogan assisted with specimen collection and care.

References

Andersen, S.O., Peter, M.G., Roepstorff, P., 1996. Cuticular sclerotization in insects. Comparative Biochemistry and Physiology 113B, 689–705.

Coleman, J.E., 1992. Zinc proteins: enzymes, storage proteins, transcription factors and replication proteins. Annual Review of Biochemistry 61, 897–946.

Compere, P., Goffinet, G., 1987a. Aspects ultrastructuraux et fonctionnels de diverses regions cuticulaires non mineralisees d'un crustace decapode, carcinus maenas. Ann Soc Royale Zoologique de Belgique 117, 159–173.

Compere, P., Goffinet, G., 1987b. Elaboration and ultrastructural changes in the pore canal system of the mineralized cuticle of *Carcinus maenas* during the moulting cycle. Tissue and Cell 19, 859–875.

Fujita, S.C., Inoue, H., Yoshioka, T., Hotta, Y., 1987. Quantitative tissue isolation from *Drosophila* freeze-dried in acetone. Biochemical Journal 243, 97–104.

Grime, G.W., Palsgard, E., Garman, E.F., Ugarte, M., Pottage, D., Wyeth, P., 1999. Recent biomedical applications of the Oxford Scanning Proton Microprobe. International Journal of PIXE 9, 199–216.

Guggenheim, K., Gaster, D., 1973. The role of manganese, copper, and zinc in the physiology of bones and teeth. In: Zipkin, I. (Ed.), Biological Mineralization. John Wiley and Sons, Inc., New York, pp. 444–462.

Holland, B., Welch, A.A., Unwin, I.D., Buss, D.H., Paul, A.A., Southgate, D.A.T., 1996. McCance and Widdowson's The Composition of Foods. The Royal Society of Chemistry, Cambridge, UK.

Hopkins, T.L., Kramer, K.J., 1992. Insect cuticle sclerotization. Annual Review of Entomology 37, 237–302.

Lowenstam, H.A., Weiner, S., 1989. On Biomineralization. Oxford University Press, Oxford, UK.

Roer, D.R., Dillman, R.M., 1993. Molt-related changes in integumental structure and function. In: Horst, M.N., Freeman, J.A. (Eds.), The Crustacean Integument, Boca Raton. CRC Press, London, pp. 1–38.

Schofield, R.M.S., 2001. Metals in cuticular structures. In: Brownell, P., Polis, G. (Eds.), Scorpion Biology and Research. Oxford University Press, Oxford, UK, pp. 234–256.

Schofield, R.M.S., 1990. X-ray microanalytic concentration measurements in unsectioned specimens: A technique and its application to Zn, Mn, and Fe enriched mechanical structures of organisms from three phyla. PhD dissertation, University of Oregon, Eugene, OR.

Schofield, R.M.S., Lefevre, H.W., 1993. Analysis of unsectioned specimens: 2D and tomographic PIXE with STIM. Nuclear Instruments and Methods in Physics Research B 77, 217–224.

Schofield, R.M.S., Postlewait, J.P., Lefevre, H.W., 1997. MeV-ION microprobe analyses of whole *Drosophila* suggest that zinc and copper accumulation is regulated storage not deposit excretion. Journal of Experimental Biology 200, 3235–3243.

Schofield, R.M.S., Lefevre, H.W., Overley, J.C., Macdonald, J.D., 1988. X-ray microanalytical surveys of minor element concentrations in unsectioned biological samples. Nuclear Instruments and Methods in Physics Research B 30, 398–403.

Schofield, R.M.S., Nesson, M., Richardson, K.A., 2002 (in press). Tooth hardness increased with zinc-content in mandibles of young leaf-cutter ants. Naturwissenschaften.

Smith, M.R., 1928. The biology of *T. sessile* Say, an important house-infesting ant. Annals of the Entomological Society of America 21, 307–329.

Smith, M.R., 1965. House-infesting ants of the eastern United States: their recognition, biology, and economic importance. US Department of Agriculture Technical bulletin 1326.

Vincent, J.W.V., 1982. Structural Biomaterials. John Wiley & Sons, New York.

Webb, J., Macey, D.J., Mann, S., 1989. Biomineralization of iron in molluscan teeth. In: Mann, S., Webb, J., Williams, R.J.P. (Eds.), Biomineralization: Chemical and Biochemical Perspectives. VCH Publishers, New York, pp. 345–388.